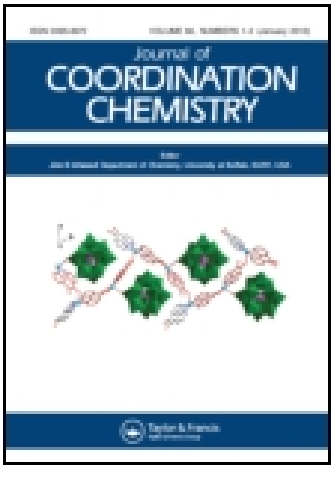

Journal of Coordination Chemistry
Publication details, including instructions for authors and subscription information:
http://www.tandfonline.com/loi/gcoo20

Two- and three-dimensional coordination complexes constructed by 2-(1H-imidazol-1-methyl)-1H-benzimidazole: syntheses, structures, and fluorescent properties

Wan-Lu Duan[a], Yu-Hong Zhang[a], Xiu-Xiu Wang[a] & Xiang-Ru Meng[a]
[a] College of Chemistry and Molecular Engineering, Zhengzhou University, Zhengzhou, PR China

Accepted author version posted online: 10 Jun 2014.Published online: 08 Jul 2014.

To cite this article: Wan-Lu Duan, Yu-Hong Zhang, Xiu-Xiu Wang & Xiang-Ru Meng (2014) Two- and three-dimensional coordination complexes constructed by 2-(1H-imidazol-1-methyl)-1H-benzimidazole: syntheses, structures, and fluorescent properties, Journal of Coordination Chemistry, 67:11, 1980-1991, DOI: 10.1080/00958972.2014.933210

To link to this article: http://dx.doi.org/10.1080/00958972.2014.933210

Journal of Coordination Chemistry, 2014
Vol. 67, No. 11, 1980–1991, http://dx.doi.org/10.1080/00958972.2014.933210

Two- and three-dimensional coordination complexes constructed by 2-(1*H*-imidazol-1-methyl)-1*H*-benzimidazole: syntheses, structures, and fluorescent properties

WAN-LU DUAN, YU-HONG ZHANG, XIU-XIU WANG and XIANG-RU MENG*

College of Chemistry and Molecular Engineering, Zhengzhou University, Zhengzhou, PR China

(*Received 19 February 2014; accepted 16 May 2014*)

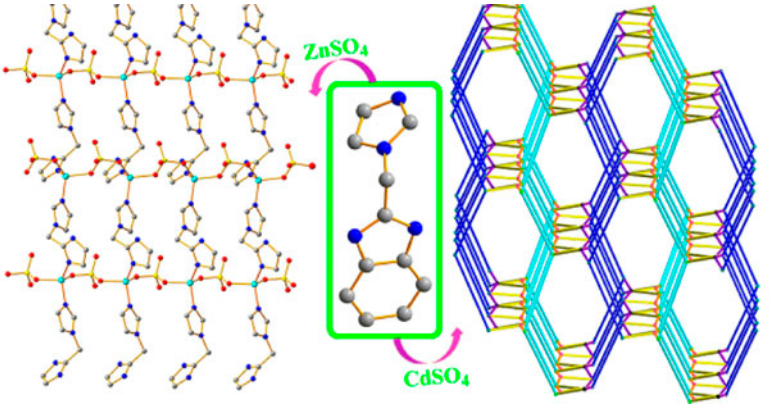

Two new complexes, $\{[Zn(imb)(SO_4)]\cdot H_2O\}_n$ (**1**) and $\{[Cd_2(imb)_2(SO_4)_2(H_2O)]\cdot CH_3OH\}_n$ (**2**), have been synthesized and characterized by single crystal X-ray diffraction. Additionally, their UV–vis, IR, Thermogravimetric analyses and fluorescent properties are also investigated.

Two new complexes, $\{[Zn(imb)(SO_4)]\cdot H_2O\}_n$ (**1**) and $\{[Cd_2(imb)_2(SO_4)_2(H_2O)]\cdot CH_3OH\}_n$ (**2**) (imb = 2-(1*H*-imidazol-1-methyl)-1*H*-benzimidazole), have been solvothermally synthesized. Single-crystal X-ray diffraction shows that **1** displays a 2-D (4,4) network, which is further extended to a 3-D supramolecular structure by hydrogen bonding interactions. Complex **2** exhibits a 3-D framework with (3,5)-connected $(4^2\cdot6)_2(4^2\cdot6^5\cdot8^3)_2$ topology. The results indicate that changing metal ions can influence the coordination modes of sulfate, and then affect the structures of the complexes. In addition, IR and UV–vis spectra, powder X-ray diffraction patterns, thermogravimetric analyses, and fluorescent properties of both complexes have been investigated.

Keywords: Zn(II) and Cd(II) complexes; Crystal structure; Fluorescence; Thermogravimetric analysis

*Corresponding author. Email: mxr@zzu.edu.cn

1. Introduction

The design of coordination polymers has attracted great attention owing to their use in gas storage and separation, catalysis, sensors, biomedicine, etc. [1–5], but it is still a challenge to predict the exact structures and compositions of the products. Generally, construction of complexes can be greatly influenced by several factors, such as the nature of the metal ions, counter ions, temperature, ligands, solvent, and metal-to-ligand ratio [6]. Selection of ligand is crucial since changing the structure of the ligand can control structures of the complexes [7, 8]. Multidentate *N*-heterocyclic flexible ligand, 2-(1*H*-imidazol-1-methyl)-1*H*-benzimidazole (imb), has been employed to construct complexes since it has three potential *N*-donors and flexible methylene spacer that can form variable coordination modes and allow for greater structural diversity [9–11]. Selection of anion is also very important for the structure of the final assembly, especially when the ligand is neutral [12]. For example, sulfate not only can keep charge balanced but it is also a polydentate ligand that can exhibit a variety of coordination modes both in solution and the solid state [13, 14]. Complexes with d^{10}-metal ions, especially zinc or cadmium, are promising candidates for photoactive materials if the ligands exhibit fluorescence [15–18].

Herein, we select the multidentate unsymmetrical *N*-heterocyclic ligand 2-(1*H*-imidazol-1-methyl)-1*H*-benzimidazole (imb) which possesses *N*-donor sites to coordinate to $ZnSO_4$ or $CdSO_4$, and obtained two new complexes $\{[Zn(imb)(SO_4)]\cdot H_2O\}_n$ (**1**) and $\{[Cd_2(imb)_2(SO_4)_2(H_2O)]\cdot CH_3OH\}_n$ (**2**). Their IR and UV–vis spectra, powder X-ray diffraction (PXRD) patterns, thermogravimetric analyses (TGA), and fluorescent properties have been determined.

2. Experimental

2.1. *General information and materials*

All chemicals were of AR grade and used without purification. IR data were recorded on a BRUKER TENSOR 27 spectrophotometer with KBr pellets from 400 to 4000 cm^{-1}. Elemental analyses (C, H, and N) were carried out on a FLASH EA 1112 elemental analyzer. PXRD patterns were recorded using CuKα radiation on a PANalytical X'Pert PRO diffractometer. TG measurements were performed by heating the sample from 30 to 800 °C at a rate of 10 °C min^{-1} in air on a NETZSCH STA 409 PC/PG differential thermal analyzer. Solid-state UV–vis diffuse reflectance spectra were obtained at room temperature using a Cary 5000 UV–vis–NIR spectrophotometer, and $BaSO_4$ was used as a 100% reflectance standard for all materials. Steady-state fluorescence measurements were performed using a F-7000 Fluorescence Spectrophotometer at room temperature in the solid state. 2-(1*H*-imidazole-1-methyl)-1*H*-benzimidazole (imb) was synthesized according to the literature method [19].

2.2. *Synthesis of* $\{[Zn(imb)(SO_4)]\cdot H_2O\}_n$ (1)

A mixture of 2-(1*H*-imidazol-1-methyl)-1*H*-benzimidazole (0.1 mM), $ZnSO_4\cdot 7H_2O$ (0.1 mM), H_2O (3 mL), and CH_3OH (1 mL) was poured into a Teflon-lined stainless steel vessel (25 mL), then the vessel was sealed and heated to 120 °C for 3 days. The autoclave was cooled to room temperature at 10 °C h^{-1}. The pH values of the solution before and after the reaction are 4.5 and 4.0, respectively. Crystals of $\{[Zn(imb)(SO_4)]\cdot H_2O\}_n$ suitable for X-ray analysis were collected. Anal. Calcd for $C_{11}H_{12}N_4O_5SZn$: C, 35.01; H, 3.18; N,

14.85%. Found: C, 34.70; H, 3.98; N, 14.15%. IR (KBr, cm^{-1}): 3506(m), 3111(m), 1625 (m), 1520(m), 1489(m), 1288(m), 748(s) cm^{-1}.

2.3. *Synthesis of {[Cd_2(imb)$_2$(SO_4)$_2$(H_2O)]·CH_3OH}$_n$ (2)*

The procedure was the same as that for **1**, except that $CdSO_4 \cdot 8/3H_2O$ (0.1 mM) was used instead of $ZnSO_4 \cdot 7H_2O$. The autoclave was cooled to room temperature at 10 °C h^{-1}. The pH values of the solution before and after the reaction are 5.5 and 5.0, respectively. Crystals of $\{[Cd_2(imb)_2(SO_4)_2(H_2O)] \cdot CH_3OH\}_n$ suitable for X-ray analysis were collected. Anal. Calcd for $C_{23}H_{26}N_8O_{10}S_2Cd_2$: C, 31.99; H, 3.01; N, 12.98%. Found: C, 32.11; H, 3.23; N, 12.50%. IR (KBr, cm^{-1}): 3466(m), 3121(s), 1624(w), 1518(s), 1451(s), 1280(m), 746(s) cm^{-1}.

2.4. *Single-crystal structure determination*

A suitable single crystal of each complex was carefully selected and glued to a thin glass fiber. Crystal structure determinations by X-ray diffraction were performed on a Rigaku Saturn 724 CCD area detector with a graphite monochromator for the X-ray source (MoKα radiation, $\lambda = 0.71073$ Å) operating at 50 kV and 40 mA. The data were collected in ω scan mode at 293(2) K; the crystal-to-detector distance was 45 mm. An empirical absorption correction was applied. The data were corrected for Lorentz-polarization effects. The structures were solved by direct methods and refined by full-matrix least-squares and difference Fourier techniques, based on F^2, using SHELXS-97 [20]. All non-hydrogen atoms were refined anisotropically. The hydrogens of imb were positioned geometrically and refined using a riding model. Hydrogens of water were found at reasonable positions in the differential Fourier map and located there. All the hydrogens were assigned with common

Table 1. Crystal data and structural refinement of **1** and **2**.

Complex	**1**	**2**
Empirical formula	$C_{11}H_{12}ZnN_4O_5S$	$C_{23}H_{26}Cd_2N_8O_{10}S_2$
Formula weight	377.68	863.44
Temperature (K)	293(2)	293(2)
Crystal system	Orthorhombic	Monoclinic
Space group	$P2_12_12_1$	$P2_1/c$
Unit cell dimensions (Å, °)		
a (Å)	4.9312(10)	15.577(3)
b (Å)	16.218(3)	15.055(3)
c (Å)	16.799(3)	13.677(3)
α (°)	90	90
β (°)	90	113.91(3)
γ (°)	90	90
V (Å^3)	1343.5(4)	2932.1(9)
Z	1	4
D_{Calcd} (g cm^{-3})	1.867	1.956
μ (mm^{-1})	2.015	1.663
F (0 0 0)	768	1712
R_{int}	0.0270	0.0299
Data/restraints/parameters	3121/0/200	6978/0/408
Goodness-of-fit on F^2	1.041	1.102
Final R indices [$I > 2\sigma(I)$]	$R_1 = 0.0411$	$R_1 = 0.0343$
	$wR_2 = 0.0877$	$wR_2 = 0.0690$
R indices (all data)	$R_1 = 0.0474$	$R_1 = 0.0409$
	$wR_2 = 0.0919$	$wR_2 = 0.0725$

Table 2. Selected bond lengths (Å) and angles (°) for **1** and **2**.

Complex **1**			
Zn(1)–O(1)	1.946(3)	Zn(1)–N(1)	1.992(3)
Zn(1)–O(2)#1	1.952(3)	Zn(1)–N(3)	2.020(3)
O(1)–Zn(1)–O(2)#1	106.48(12)	O(1)–Zn(1)–N(1)	110.63(14)
O(2)#1–Zn(1)–N(1)	101.94(13)	O(1)–Zn(1)–N(3)	111.08(14)
O(2)#1–Zn(1)–N(3)	111.29(14)	N(1)–Zn(1)–N(3)	114.77(12)
Complex **2**			
Cd(1)–N(1)	2.238(2)	Cd(1)–N(4)#1	2.249(2)
Cd(1)–O(5)	2.311(2)	Cd(1)–O(2)	2.330(3)
Cd(1)–O(8)#2	2.382(2)	Cd(1)–O(1)	2.597(3)
Cd(2)–N(5)	2.259(2)	Cd(2)–O(6)#2	2.268(2)
Cd(2)–O(9)	2.342(2)	Cd(2)–O(3)	2.366(2)
Cd(2)–N(8)#3	2.316(2)	Cd(2)–O(4)#2	2.390(2)
N(1)–Cd(1)–N(4)#1	109.56(10)	N(5)–Cd(2)–O(6)#2	92.54(9)
N(4)#1–Cd(1)–O(5)	94.96(8)	N(5)–Cd(2)–O(9)	175.14(9)
O(5)–Cd(1)–O(2)	106.18(9)	N(5)–Cd(2)–O(3)	86.83(8)
N(1)–Cd(1)–O(8)#2	83.30(8)	O(9)–Cd(2)–O(3)	88.37(8)
O(5)–Cd(1)–O(8)#2	163.06(8)	N(8)#3–Cd(2)–O(4)#2	90.92(8)
O(2)–Cd(1)–O(8)#2	90.75(9)	O(6)#2–Cd(2)–N(8)#3	167.56(8)
O(5)–Cd(1)–O(1)	84.59(8)	N(8)#3–Cd(2)–O(3)	92.94(9)
O(8)#2–Cd(1)–O(1)	104.79(8)	O(3)–Cd(2)–O(4)#2	173.71(8)
N(1)–Cd(1)–O(5)	81.29(8)	N(5)–Cd(2)–N(8)#3	99.56(9)
N(1)–Cd(1)–O(2)	152.41(9)	O(6)#2–Cd(2)–O(9)	86.78(7)
N(4)#1–Cd(1)–O(2)	96.42(9)	O(6)#2–Cd(2)–O(3)	90.61(8)
N(4)#1–Cd(1)–O(8)#2	83.61(8)	N(5)–Cd(2)–O(4)#2	87.64(9)
N(4)#1–Cd(1)–O(1)	151.14(8)	O(9)–Cd(2)–O(4)#2	97.12(8)
N(1)–Cd(1)–O(1)	98.92(9)	N(8)#3–Cd(2)–O(9)	81.41(8)
O(2)–Cd(1)–O(1)	56.56(8)	O(6)#2–Cd(2)–O(4)#2	86.67(8)

Notes: Symmetry transformations used to generate equivalent atoms: For **1**: #1: $x+1$, y, z. For **2**: #1: $1-x$, $y+0.5$, $1.5-z$; #2: x, $1.5-y$, $z-0.5$; #3: $2-x$, $y-0.5$, $1.5-z$.

Table 3. Hydrogen bonds of **1** and **2**.

D–H···A	*d*(D–H) (Å)	*d*(H···A) (Å)	*d*(D···A) (Å)	(D–H···A) (°)
Complex **1**				
O(5)–H(1W)···O(3)	0.85	2.12	2.964(6)	170.4
O(5)–H(2W)···O(3)#2	0.85	2.43	3.220(6)	154.0
N(4)–H(4C)···O(3)#5	0.86	1.97	2.798(4)	160.4
Complex **2**				
N(7)–H(7B)···O(10)	0.86	2.07	2.764(4)	137.0
O(9)–H(2W)···O(1)	0.85	1.98	2.739(3)	147.5
N(3)–H(3B)···O(7)#2	0.86	1.92	2.753(3)	163.8
O(9)–H(1W)···O(7)#2	0.85	1.84	2.671(3)	166.7
O(10)–H(10)···O(1)#2	0.82	2.36	2.788(4)	113.7

Notes: Symmetry transformations used to generate equivalent atoms: For **1**: #2: $x-1$, y, z; #5: $-x-0.5$, $1-y$, $z-0.5$. For **2**: #2: x, $1.5-y$, $z-0.5$.

isotropic displacement factors and included in the final refinement. Crystallographic parameters and structural refinement for the complexes are summarized in table 1. Selected bond lengths and angles are listed in table 2. Hydrogen bonds are listed in table 3. CCDC reference numbers are 982624 and 982625 for **1** and **2**, respectively.

3. Results and discussion

3.1. *IR spectra*

IR spectra show that absorptions at 3506 cm^{-1} for **1** and 3466 cm^{-1} for **2** are attributed to O–H stretch. Absorptions at 3111 cm^{-1} for **1** and 3121 cm^{-1} for **2** originate from C(arene)–H stretch. Three sharp absorptions at 1625, 1520, and 1489 cm^{-1} for **1** and 1624, 1518, and 1451 cm^{-1} for **2** could be associated with the stretching vibrations of C=C and C=N. The absorption bands of 1288 cm^{-1} for **1** and 1280 cm^{-1} for **2** are due to C–N stretch. Absorptions at 748 cm^{-1} for **1** and 746 cm^{-1} for **2** correspond to characteristic stretching vibrations of 1,2-substituted benzene rings. The above analyses are confirmed by the results of the X-ray diffraction.

3.2. *Crystal structure of {[Zn(imb)(SO_4)]·H_2O}$_n$ (1)*

Single-crystal X-ray analysis revealed that **1** crystallizes in orthorhombic space group $P2_12_12_1$. As depicted in figure 1(a), the asymmetric unit contains one Zn(II), one imb ligand, one sulfate, and one uncoordinated water. Each Zn(II) is in a slightly distorted tetrahedral coordination environment with two nitrogens (N1, N3) from two imb ligands and two oxygens (O1, O2#1) from two sulfates. The bond lengths of Zn–N are 1.992(3) and 2.020(3) Å, and the Zn–O bond lengths are 1.946(3) and 1.952(3) Å. These bond lengths are close to those in reported Zn(II) complexes, such as [Zn_2(η^2-O_2CFcCO_2)$_2$(2,2′-bpy)$_2$(H_2O)$_2$]·CH_3OH·H_2O [21]. The bond angles around Zn(II) range from 101.94(13)° to 114.77(12)°. In **1**, each imb ligand bridges two Zn(II) ions forming a ···Zn–imb–Zn··· chain parallel to the crystallographic *b* direction, and the chains are further linked by bridging sulfates to give a 2-D layered network containing quadrangular grid units [figure 1(b)]. Each grid is constructed by two imb ligands and two sulfates acting as the four edges and four Zn(II) ions acting as the four vertices giving a 22-membered metallocyclic ring. The diagonal distances are 9.3332(14) × 9.6871(14) Å. In addition, there are two kinds of O–H···O hydrogen bonds between uncoordinated water and sulfate, and one kind of N–H···O hydrogen bond between imb and sulfate. Adjacent layers with distance of ca. 8.5 Å are stacked via the above three kinds of hydrogen bonds leading to a 3-D structure [figure 1(c)]. As shown in figure S1 (see online supplemental material at http://dx.doi.org/10.1080/00958972.2014.933210), the 3-D framework has solvent-accessible porosities of which the volume is approximately 119.6 $Å^3$ per unit cell (1343.5 $Å^3$), being equal to about 8.9% of the total crystal volume estimated by PLATON.

3.3. *Crystal structure of {[Cd_2(imb)$_2$(SO_4)$_2$(H_2O)]·CH_3OH}$_n$ (2)*

When $CdSO_4$·8/3H_2O, instead of $ZnSO_4$·7H_2O, is used with the other experimental conditions unchanged, **2** is obtained. Complex **2** displays a 3-D framework which is different from **1**, and water molecules coordinated to Cd(II). As the radius of Cd(II) is larger than that of Zn(II), Cd(II) in **2** is six-coordinate. Single-crystal X-ray diffraction analysis reveals that **2** crystallizes in the monoclinic $P2_1/c$ space group. There are two Cd(II) ions, two imb ligands, two sulfates, one coordinated water, and one uncoordinated methanol in the asymmetric unit of **2**. As illustrated in figure 2(a), both Cd1 and Cd2 adopt slightly distorted octahedral coordination. Each Cd1 is six-coordinate with four oxygens from three sulfate, and two nitrogens from two imb ligands. The five nearly coplanar atoms O1, O2, N1, N4#1, and Cd1 form an equatorial plane (the mean deviation from plane is 0.1452 Å), while O5

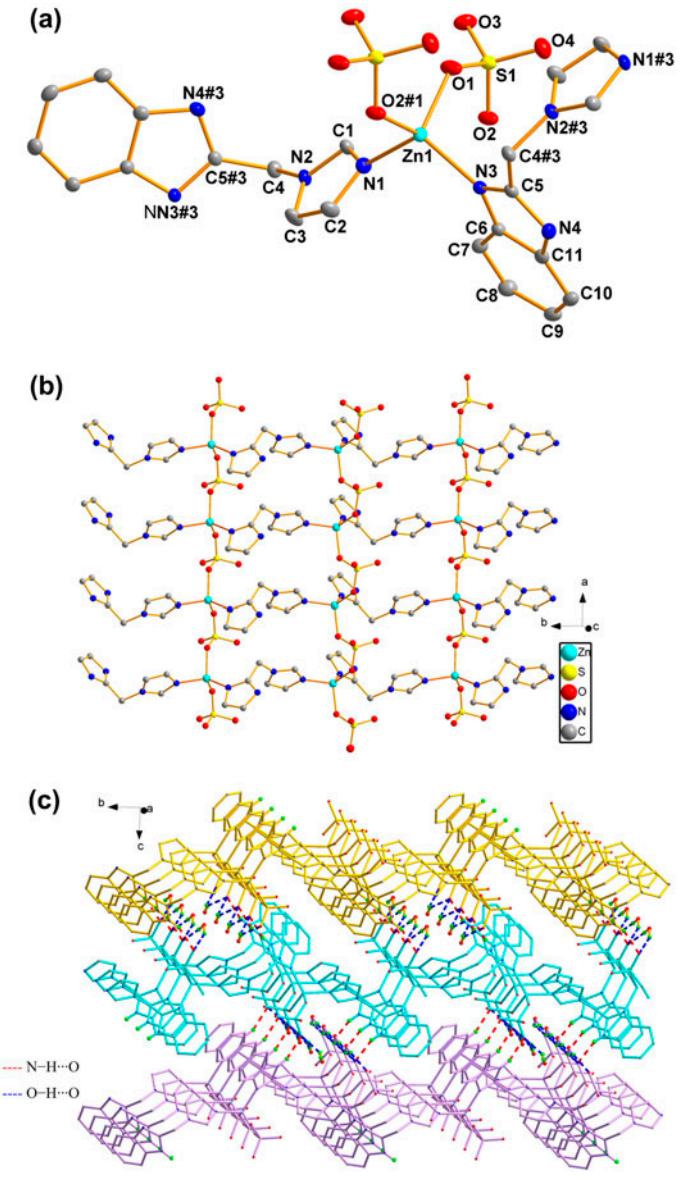

Figure 1. (a) Coordination environment of Zn(II) in **1** with ellipsoids drawn at the 30% probability level; the hydrogens and uncoordinated waters have been omitted for clarity. (b) View of the 2-D layered network in **1** along the *c*-axis; part of the benzene rings have been omitted for clarity. (c) 3-D structure of **1** linked through hydrogen-bonding indicated by dashed lines.

and O8#2 occupy axial positions with the O5–Cd1–O8#2 bond angle of 163.06(8)°. The coordination environment of Cd2 is different from Cd1. Cd2 bonds three oxygens from three sulfate anions, one oxygen from coordinated water molecule, and two nitrogens from two imb ligands. The axial positions are occupied by O3 and O4#2 with the O3–Cd2–O4#2 bond angle of 173.71(8)°; N5, N8#3, O9, O6#2, and Cd2 are almost located in the same plane (the mean deviation from plane is 0.0680 Å). As shown in table 2, the Cd–O and

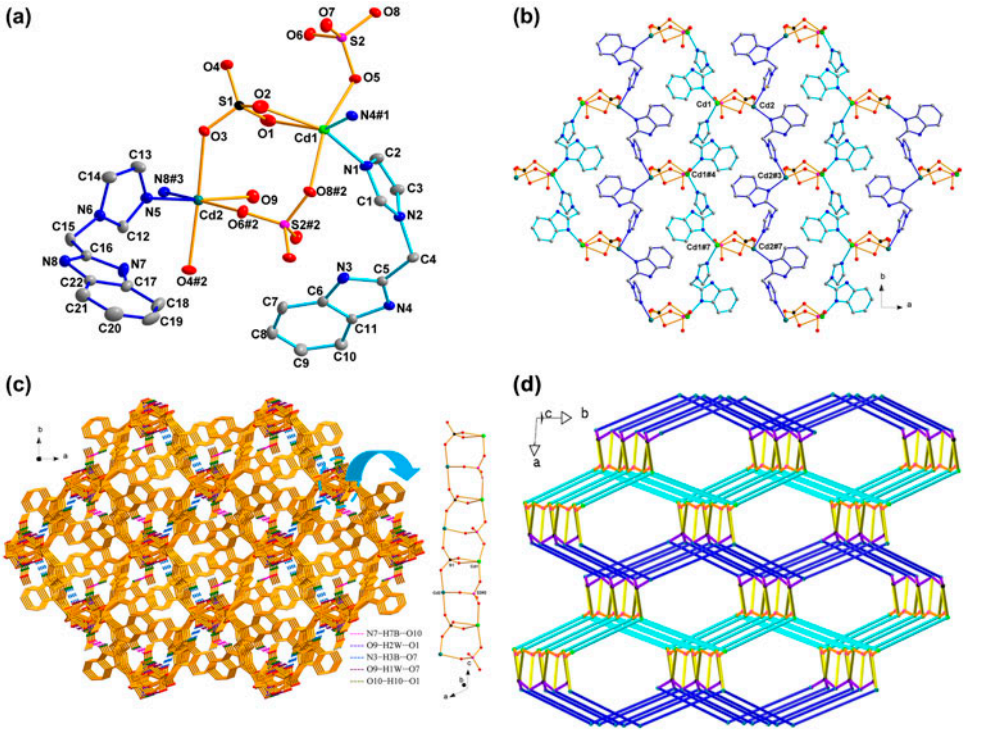

Figure 2. (a) ORTEP drawing of the coordination environments of Cd1 and Cd2 in **2** with the ellipsoids drawn at the 30% probability level; all hydrogens and uncoordinated methanol molecules are omitted for clarity. (b) The illustration of single 2-D layer in the *ab* plane (the coordinated waters and uncoordinated methanols are omitted for clarity). (c) View of the 3-D framework along the *c*-axis. (d) Schematic illustration of the topology of **2**. Color code: green balls, Cd1; teal balls, Cd2; black balls, S(1)O_4; pink balls, S(2)O_4; blue sticks, imb (N5); turquoise sticks, imb (N1) (see http://dx.doi.org/10.1080/00958972.2014.933210).

Cd–N bond lengths in **2** are longer than the Zn–O and Zn–N bond lengths in **1** due to the bigger radius of Cd(II) in comparison to that of Zn(II), but are close to the Cd–O and Cd–N bond lengths in the reported Cd(II) complexes [Cd(BDC)(phen)·DMF] (H_2BDC = benzene-1,4-dicarboxylic acid, phen = 1,10-phenanthroline) [22] and [Cd(Htmb)$_2$(Cl)$_2$(H_2O)$_2$]·4H_2O (Htmb = 2-((1*H*-triazol-1-yl)methyl)-1*H*-benzimidazole) [23]. There are two crystallographically independent sulfates in **2** and they coordinate to Cd(II) with modes II and III (scheme 1), while all of the sulfates are equivalent and coordinate to Zn(II) with mode I (scheme 1) in **1**. One kind of sulfate is a 3-connector coordinated with one Cd2 and two Cd1 ions in O-,O-,O-monodentate fashion (mode II); the other sulfate as a 3-connector links to one Cd1 in bis-O,O-chelating and two Cd2 ions in O-,O-monodentate fashion (mode III). Cd(II) ions are connected by the two kinds of sulfate anions to form a [$Cd_2(SO_4)_2$] dinuclear unit with Cd1···Cd2 distance of 4.9714(11) Å [figure 2(a)]. In addition, there are also two kinds of imb ligands. One kind of imb (N1) bridge Cd1 ions and the other kind of imb (N5) link Cd2 ions. [$Cd_2(SO_4)_2$] binuclear units are joined by two kinds of imb ligands generating a 2-D layer parallel to the *ab*-plane [figure 2(b)]. As shown in figure 2(c), along the *c* axis, adjacent layers are further linked by the two kinds of sulfate anoins resulting in a 3-D framework. The total solvent-accessible volume for **2** was approximately 307.2 Å^3 per unit cell (2932.1 Å^3), being equal to about 10.5% of the total crystal volume estimated by PLATON.

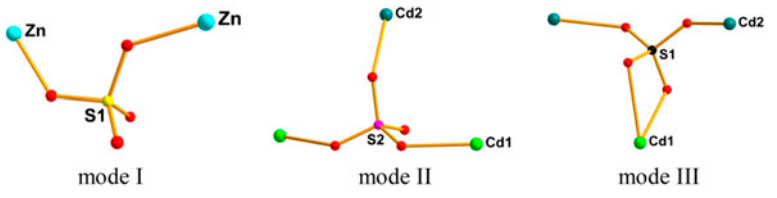

Scheme 1. Coordination modes of sulfate anion found in **1** (mode I) and **2** (modes II and III).

Figure S2 (Supplementary material) shows the porosities in **2**. If the imb is considered as a single linker, the sulfate is considered as a three-connected node, and Cd(II) can be viewed as a five-connected node, and uncoordinated methanol molecules are omitted, the overall structure of **2** can be classified as a (3,5)-connected $(4^2{\cdot}6)_2(4^2{\cdot}6^5{\cdot}8^3)_2$ topology [figure 2(d)]. As shown in table 3, there exist three kinds of O–H···O hydrogen bonds among coordinated water, sulfate, and methanol, and two kinds of N–H···O hydrogen bonds among imb ligands, sulfate anions, and methanol molecules. These hydrogen bonds stabilize the structure of **2**.

3.4. *PXRD patterns and TGA*

PXRD experiments were carried out for **1** and **2**. The patterns for the as-synthesized bulk materials closely match the simulated ones from the single-crystal structure analysis, which are indicative of pure solid-state phases (figure 3). TGA of **1** and **2** were performed by heating the sample from 30 to 800 °C in air (figure 4). Complex **1** is stable to 72 °C and the first mass loss of 4.56% occurs from 72 to 230 °C, corresponding to the release of uncoordinated water (Calcd 4.77%). Then a plateau region is observed from 230 to 378 °C. Continuous mass loss from 378 to 671 °C corresponds to gradual decomposition of the sulfate and imb ligands. Finally, a plateau occurs from 671 to 800 °C. The remaining weight corresponded to the formation of ZnO (observed 22.16%, Calcd 21.55%). The PXRD pattern of the residue (figure S3 in Supplementary material) is consistent with the standard of ZnO (JCPDS: 75-576). Complex **2** showed a weight loss of 3.74% from 43 to 85 °C, which was attributed to release of uncoordinated CH_3OH molecules (Calcd 3.71%). Then a plateau region is observed from 85 to 177 °C. Continuous mass loss of 2.08% from 177 to 243 °C corresponds to the release of coordinated water (Calcd 2.1%). The framework of **2** started to decompose when the temperature was higher than 243 °C. Finally a plateau occurs from 684 to 800 °C. The remaining weight corresponded to the formation of CdO (observed 29.82%, Calcd 29.74%). The PXRD pattern of the residue (figure S3) is consistent with the standard of CdO (JCPDS: 5-640).

3.5. *Luminescent properties*

A number of complexes with d^{10} metal centers have been investigated for fluorescence properties because of their potential applications in photochemistry, chemical sensors, and electroluminescent displays [24]. The luminescent properties of **1**, **2**, and free imb were examined in the solid state at room temperature, as illustrated in figure 5. The free imb displays a fluorescent emission band at $\lambda_{max} = 305$ nm upon excitation at 271 nm, which can be attributable to $\pi^* \rightarrow \pi$ transition of imb. Intense bands were observed at 313 nm for **1** and 336 nm for **2** under the excitation at 271 nm. The emission spectra of **1** and **2** are very

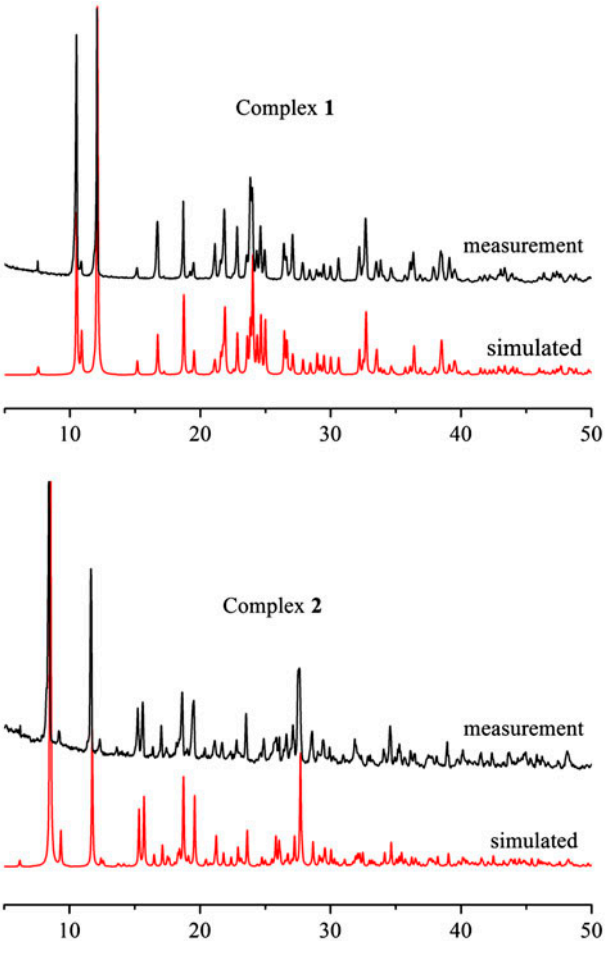

Figure 3. The PXRD patterns of **1** and **2** at room temperature; simulated patterns are generated from single-crystal diffraction data.

similar to that of imb, demonstrating that the emission spectra of **1** and **2** are attributed to an intraligand emission state [25]. The fluorescence curves of **1** and **2** present more or less bathochromic shift in contrast to that of imb, which should be attributed to the metal–ligand coordination interaction [26]. The ligands and metal ions make contributions to the luminescent properties simultaneously.

3.6. *UV–vis absorption spectra*

The UV–vis absorption spectra of free imb, **1**, and **2** were obtained in the crystalline state at room temperature. As shown in figure S4 (Supplementary material), imb shows intense absorption peaks at 220−300 nm, which can be ascribed to $\pi^* \rightarrow \pi$ transition of the ligand. Lower energy bands of **1** and **2** from 350 to 500 nm are probably assigned as metal-to-ligand charge-transfer transition [27].

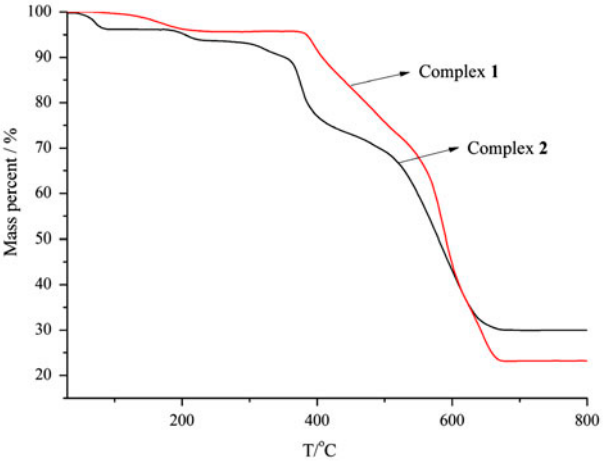

Figure 4. TGA curves of **1** and **2**.

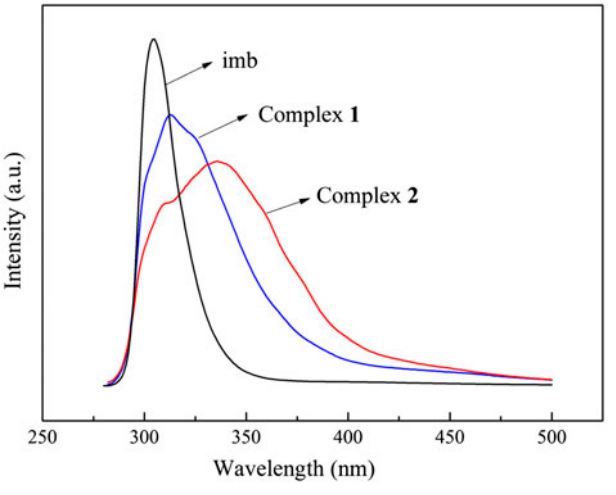

Figure 5. Solid-state emission spectra of imb, **1** and **2** at room temperature.

4. Conclusion

Due to Zn(II) or Cd(II) coordination to *N* and *O*-donors simultaneously, most of the Zn(II) or Cd(II) complexes are obtained by using mix-ligands of *N*-heterocyclic compounds and polycarboxylates [28–39], and some other complexes are constructed through using one type of ligand, such as *N*-heterocyclic ligand [40–44]. Here, we use one type of *N*-heterocyclic ligand 2-(1*H*-imidazol-1-methyl)-1*H*-benzimidazole to assemble with $ZnSO_4$ or $CdSO_4$ and obtain two new complexes $\{[Zn(imb)(SO_4)]\cdot H_2O\}_n$ (**1**) and $\{[Cd_2(imb)_2(SO_4)_2(H_2O)]\cdot CH_3OH\}_n$ (**2**). Complex **1** displays a 2-D (4,4) network in which all of the sulfates coordinate to Zn(II) with mode I (scheme 1), whereas **2**

exhibits a 3-D framework in which two kinds of sulfates coordinate to Cd(II) with modes II and III (scheme 1). These results suggest that the change of metal ions can influence the coordination modes of sulfate, and then affect the structures of the complexes, and finally lead to the different properties.

Supplementary material

Crystallographic data reported in this article have been deposited with the Cambridge Crystallographic Data Center as supplementary publication. CCDC numbers are 982624–982625. These data can be obtained free of charge via http://www.ccdc.cam.ac.uk/conts/retrieving.html (or from the Cambridge Crystallographic Data Center, 12 Union Road, Cambridge CB2 1EZ, UK; Fax: +44 1223 336 033).

Funding

We gratefully acknowledge the financial support by the National Natural Science Foundation of China [grant number J1210060].

References

[1] (a) M.P. Suh, H.J. Park, T.K. Prasad, D.W. Lim. *Chem. Rev.*, **112**, 782 (2012); (b) K. Sumida, D.L. Rogow, J.A. Mason, T.M. McDonald, E.D. Bloch, Z.R. Herm, T.H. Bae, J.R. Long. *Chem. Rev.*, **112**, 724 (2012).
[2] J.R. Li, J. Sculley, H.C. Zhou. *Chem. Rev.*, **112**, 869 (2012).
[3] M. Yoon, R. Srirambalaji, K. Kim. *Chem. Rev.*, **112**, 1196 (2012).
[4] L.E. Kreno, K. Leong, O.K. Farha, M. Allendorf, R.P. Van Duyne, J.T. Hupp. *Chem. Rev.*, **112**, 1105 (2012).
[5] P. Horcajada, R. Gref, T. Baati, P.K. Allan, G. Maurin, P. Couvreur, G. Férey, R.E. Morris, C. Serre. *Chem. Rev.*, **112**, 1232 (2012).
[6] (a) B. Chen, M. Eddaoudi, T.M. Reineke, J.W. Kampf, M. O'Keeffe, O.M. Yaghi. *J. Am. Chem. Soc.*, **122**, 11559 (2000); (b) A. Galet, M.C. Munoz, J.A. Real. *J. Am. Chem. Soc.*, **125**, 14224 (2003); (c) M. Dinca, A.F. Yu, J.R. Long. *J. Am. Chem. Soc.*, **128**, 8904 (2006); (d) D. Li, T. Wu, X.P. Zhou, R. Zhou, X.C. Huang. *Angew. Chem. Int. Ed.*, **44**, 4175 (2005).
[7] J. Fan, H.F. Zhu, T.A. Okamura, W.Y. Sun, W.X. Tang, N. Ueyama. *Inorg. Chem.*, **42**, 158 (2003).
[8] H.K. Liu, W.Y. Sun, D.J. Ma, K.B. Yu, W.X. Tang. *Chem. Commun.*, 591 (2000).
[9] S.X. Yan, D. Zhao, T. Li, R. Wang, X.R. Meng. *J. Coord. Chem.*, **65**, 945 (2012).
[10] X.X. Wang, M. Yu, T. Li, X.R. Meng. *Inorg. Chem. Commun.*, **40**, 187 (2014).
[11] Y.T. Wang, G.M. Tang, Y.Q. Wei, T.X. Qin, T.D. Li, C. He, J.B. Ling, X.F. Long, S.W. Ng. *Cryst. Growth Des.*, **10**, 25 (2010).
[12] Y.M. Lee, S.J. Hong, H.J. Kim, S.H. Lee, H. Kwak, C. Kim, S.J. Kim, Y. Kim. *Inorg. Chem. Commun.*, **10**, 287 (2007).
[13] C. Papatriantafyllopoulou, E. Manessi-Zoupa, A. Escuer, S.P. Perlepes. *Inorg. Chim. Acta*, **362**, 634 (2009).
[14] R.E. Wilson. *Inorg. Chem.*, **51**, 8942 (2012).
[15] C.Y. Yue, C.F. Yan, R. Feng, M.Y. Wu, L. Chen, F.L. Jiang, M.C. Hong. *Inorg. Chem.*, **48**, 2873 (2009).
[16] M.D. Allendorf, C.A. Bauer, R.K. Bhaktaa, R.J.T. Houka. *Chem. Soc. Rev.*, **38**, 1330 (2009).
[17] J.Y. Hu, J.A. Zhao, Q.Q. Guo, H.W. Hou, Y.T. Fan. *Inorg. Chem.*, **49**, 3679 (2010).
[18] X.Q. Yao, D.P. Cao, J.S. Hu, Y.Z. Li, Z.J. Guo, H.G. Zheng. *Cryst. Growth Des.*, **11**, 231 (2011).
[19] A.R. Katritzky, M. Drewniak-Deyrup, X.F. Lan, F. Brunner. *J. Heterocycl. Chem.*, **26**, 829 (1989).
[20] G.M. Sheldrick. *Acta Cryst.*, **A64**, 112 (2008).
[21] X. Meng, H. Hou, G. Li, B. Ye, T. Ge, Y. Fan, Y. Zhu, H. Sakiyama. *J. Organomet. Chem.*, **689**, 1218 (2004).
[22] X. Shi, G.S. Zhu, X.H. Wang, G.H. Li, Q.R. Fang, G. Wu, G. Tian, M. Xue, X.J. Zhao, R.W. Wang, S.H. Qiu. *Cryst. Growth Des.*, **5**, 207 (2005).
[23] W.J. Chu, X.H. Lou, Z.Y. Wang, C.Y. Xu, Y.T. Fan, H.W. Hou. *J. Coord. Chem.*, **64**, 4373 (2011).

[24] (a) E.Y. Lee, S.Y. Jang, M.P. Suh. *J. Am. Chem. Soc.*, **127**, 6374 (2005); (b) Q.G. Wu, M. Esteghamatian, N.X. Hu, Z. Popovic, G. Enright, Y. Tao, M. D'Iorio, S.N. Wang. *Chem. Mater.*, **12**, 79 (2000); (c) Y.H. He, Y.L. Feng, Y.Z. Lan, Y.H. Wen. *Cryst. Growth Des.*, **8**, 3586 (2008).
[25] (a) Y. Gong, W. Tang, W.B. Hou, Z.Y. Zha, C.W. Hu. *Inorg. Chem.*, **45**, 4987 (2006); (b) M.S. Wang, G.C. Guo, M.L. Fu, L. Xu, L.Z. Cai, J.S. Huang. *Dalton Trans.*, 2899 (2005); (c) W. Chen, J.Y. Wang, C. Chen, Q. Yue, H.M. Yuan, J.S. Chen, S.N. Wang. *Inorg. Chem.*, **42**, 944 (2003).
[26] O.S. Wolfbeis. *Fluorescence Methods and Applications: Spectroscopy, Imaging, and Probes*, Wiley-Blackwell, Hoboken, NJ (2008).
[27] J.H. Cui, Z.Z. Lu, Y.Z. Li, Z.J. Guo, H.G. Zheng. *Cryst. Growth Des.*, **12**, 1022 (2012).
[28] J.C. Jin, W.Q. Tong, C.G. Xie, W.G. Chang, G.N. Xu, J. Wu, L.G. Li, Z.Q. Yan, Y.Y. Wang. *J. Coord. Chem.*, **66**, 3697 (2013).
[29] Z.W. Wang, M. Yu, T. Li, X.R. Meng. *J. Coord. Chem.*, **66**, 4163 (2013).
[30] H.W. Kuai, X.C. Cheng, X.H. Zhu. *J. Coord. Chem.*, **66**, 2970 (2013).
[31] J.K. Xu, X.C. Sun, C.X. Ju, L.R. Yang, C.F. Bi, M. Sun. *J. Coord. Chem.*, **66**, 2693 (2013).
[32] J.K. Xu, X.C. Sun, C.X. Ju, J. Sheng, F. Wang, M. Sun. *J. Coord. Chem.*, **66**, 2541 (2013).
[33] X.F. Wang, X.Y. Yu, J.K. Hu, H. Zhang. *J. Coord. Chem.*, **66**, 2118 (2013).
[34] Z.M. Man, F. Guo. *J. Coord. Chem.*, **66**, 1 (2013).
[35] B.T. Liu, D. Zhao, T. Li, X.R. Meng. *J. Coord. Chem.*, **66**, 139 (2013).
[36] F. Guo. *J. Coord. Chem.*, **65**, 4005 (2012).
[37] C.Z. Li, X.R. Huang, Y.H. Chen. *J. Coord. Chem.*, **65**, 3699 (2012).
[38] S.W. Jin, D.Q. Wang, Y.C. Xu. *J. Coord. Chem.*, **65**, 1953 (2012).
[39] Q.Y. Huang, W.P. Tang, C.L. Liu, X. Su, X.R. Meng. *J. Coord. Chem.*, **67**, 149 (2014).
[40] X. Su, T. Li, Y. Xiu, X.R. Meng. *Z. Naturforsch. B*, **67b**, 678 (2012).
[41] B.F. Huang, H. Huang, H.P. Xiao, J.G. Wang, X.H. Li, A. Morsali. *J. Coord. Chem.*, **65**, 3605 (2012).
[42] C.H. Jiao, C.H. He, J.C. Geng, G.H. Cui. *J. Coord. Chem.*, **65**, 2852 (2012).
[43] C.H. He, C.H. Jiao, J.C. Geng, G.H. Cui. *J. Coord. Chem.*, **65**, 2294 (2012).
[44] T. Li, X. Su, Y. Xiu, X.R. Meng. *J. Coord. Chem.*, **65**, 1792 (2012).